BMC Microbiology

RESEARCH

Open Access

Comparative genomics and evolutionary insights into zeaxanthin biosynthesis in two novel *Flavobacterium* species

Ye Zhuo[1,2†], Chun-Zhi Jin[1†], Chang-Soo Lee[3], Kee-Sun Shin[4] and Hyung-Gwan Lee[1,2*]

Abstract

Background During the screening of pigment-producing microbes from domestic sources, 102 yellow- or orange-pigmented bacteria were isolated. Among these, two novel *Flavobacterium* strains, *F. sedimentum* SUN046^T and *F. fluvius* SUN052^T, were identified as zeaxanthin producers. A polyphasic taxonomic characterization, combined with comparative genomic analysis of 45 *Flavobacterium* species, was conducted to determine their taxonomic positions and explore potential evolutionary relationships in zeaxanthin biosynthesis.

Results Both strains utilized the mevalonic acid (MVA) pathway and possessed the *crt* gene cluster (*crtB*, *crtI*, *crtY/crtY*$_{cd}$, and *crtZ*). Strain SUN046^T exhibited unique features in the carotenoid biosynthesis pathway, notably the absence of HMG-CoA synthase (HMGCS) in the upper MVA pathway and the presence of the rare lycopene *β*-cyclase *crtY*$_{cd}$, which is uncommon among bacteria. The *CrtY*$_{cd}$ in SUN046^T possessed a single active site and direct lycopene-binding modes. Conversely, *CrtY* in SUN052^T exhibited multiple active sites, which is flavin adenine dinucleotide (FAD) dependent. These structural differences has impacted catalytic efficiencies, as evidenced by zeaxanthin yields of 6.49 μg/mL in SUN046^T and 13.23 μg/mL in SUN052^T. Variations in carotenoid biosynthetic pathway among other *Flavobacterium* species were also observed.

Conclusion These findings suggest that both strains represent valuable new resources for zeaxanthin production and provide foundational insights for biotechnological applications involving the genus *Flavobacterium*, highlighting the genetic and evolutionary complexity of microbial carotenoid biosynthesis.

Keywords *Flavobacterium*, Zeaxanthin, Carotenoids, Lycopene β-cyclase, Taxonomy, Mevalonic acid (MVA) pathway

†Ye Zhuo and Chun-Zhi Jin contributed equally to this work.

*Correspondence:
Hyung-Gwan Lee
trustin@kribb.re.kr
[1]Cell Factory Research Center, Korea Research Institute of Bioscience and Biotechnology (KRIBB), 125 Gwahak-ro, Yuseong-gu, Daejeon 34141, Republic of Korea
[2]Department of Biotechnology, KRIBB School of Bioscience, Korea University of Science and Technology (UST), 217 Gajeong-ro, Yuseong-gu, Daejeon 34113, Republic of Korea
[3]Fungi Research Division, Microbial Research Department, Nakdonggang National Institute of Biological Resources, Sangju 37242, Republic of Korea
[4]Microbiome Convergence Research Center, Korea Research Institute of Bioscience and Biotechnology (KRIBB), 125 Gwahak-ro, Yuseong-gu, Daejeon 34141, Republic of Korea

Background

Carotenoids are diverse group of pigments that are widely distributed and found in bacteria, fungi, algae, and plants [1]. These pigments exhibit a range of orange, yellow, and red colors, resulting from variations in their chemical structures [2]. Distinct chemical configurations of carotenoids contribute to their diverse functions, such as antioxidant activity [3], antimicrobial properties [4], potential anti-carcinogenic [5], anti-inflammatory, antidiabetic, and Alzheimer's disease-preventative effects [6, 7]. Due to these benefits, carotenoids are extensively applied in industries including food, pharmaceuticals, animal feed, and cosmetics [8]. Carotenoid-rich foods are nutritionally valuable, as they can serve as precursors to vitamin A or act as antioxidants, with their intake associated with a reduced risk of skin cancer, chronic diseases, and cardiovascular conditions [9].

Among carotenoids, zeaxanthin (3,3'-dihydroxy-β-carotene, $C_{40}H_{56}O_2$) stands out for its unique role as an anti-photosensitizer, filtering blue light to protect eye tissues from sunlight damage. It is worth noting that animals and humans must obtain zeaxanthin through diet because they cannot synthesize it endogenously [10]. However, extracting zeaxanthin from algae and plants is a complex and costly process [11], with challenges including waste generation, low extraction efficiency and yield, instability and environmental impact [12, 13]. Therefore, microbial production of zeaxanthin has gained interest, as bacteria can synthesize it more efficiently through simpler processes (Zafar et al., 2021).

The genus *Flavobacterium*, a member of the family *Flavobacteriaceae*, was first established by Bergey et al. [14] and has since been expanded upon by various researchers [15–18]. Currently, there are 313 recognized *Flavobacterium* species with valid names, according to the List of Prokaryotic Names with Standing in Nomenclature (https://lpsn.dsmz.de/genus/Flavobacterium). Most *Flavobacterium* strains display yellow to orange coloration due to flavonoid pigments or carotenoids. Some strains mainly produce zeaxanthin as their sole pigment and their production has been improved by the application of genetic engineering, especially targeting lycopene β-cyclase, which is a key enzyme in the carotenoid biosynthesis pathway responsible for producing γ-carotene and β-carotene. Three types of lycopene β-cyclase are known: CrtY (or CrtL), heterodimeric and CruA/CruP-type (Göttl et al., 2023). Among them, CrtY is the predominant isozyme in Gram-negative bacteria. Notably, $CrtY_{cd}$, a fusion of bacterial $CrtY_c$ and $CrtY_d$ in a heterodimeric structure, was reported in *Algoriphagus* sp. KK10202C which produces flexixanthin through genes (*crtB*, *crtI*, $crtY_{cd}$ and *crtW*) involved in flexixanthin biosynthesis [19]. The $crtY_{cd}$ gene has also been identified in halophilic archaea (such as *Natronomonas*, *Halobacterium* and *Haloarcula*) and halophilic bacteria [20]. Studies have shown that although the similarity between $CrtY_{cd}$ and CrtY is relatively low, $CrtY_{cd}$ is also located in the carotenoid biosynthesis gene cluster and plays a similar function to CrtY [21].

Using a comprehensive multiphase phenotyping approach, we characterized two novel *Flavobacterium* strains, designated *Flavobacterium sedimentum* SUN046^T and *Flavobacterium fluvius* SUN052^T. Genomic comparative studies of their carotenoid biosynthesis pathways with closely related *Flavobacterium* species revealed distinct characteristics, primarily differentiated by two evolutionary patterns: the presence or absence of HMGCS (Hydroxymethylglutaryl-CoA synthase) in the upper MVA pathway and variations in lycopene cyclase (CrtY or $CrtY_{cd}$). This study examines the effects of different lycopene β-cyclase genes on zeaxanthin biosynthesis in the two isolates through conserved domain analysis, protein structure prediction, and molecular docking analysis. The findings offer new insights into microbial diversity within ecosystems and provide a foundation for exploring the biotechnological potential of the genus *Flavobacterium*, especially concerning microbial carotenoid synthesis.

Methods

Microbe isolation, preservation, and culture conditions

The strains SUN046^T and SUN052^T were isolated from water samples collected at Daechicheon and Yongso Waterfall in South Korea. Standard dilution plating techniques were applied, followed by plating onto R2A agar plates and incubation at 28 °C for five days. After incubation, individual yellow colonies were isolated. Reference strains (*F. koreense* KACC 14969^T, *F. chungnamense* KACC 14971^T, and *F. aquatile* KACC 11692^T) were obtained from the Korean Agricultural Culture Collection (KACC). SUN046^T and SUN052^T were deposited in the Korean Collection for Type Cultures (KCTC), Freshwater Bioresources Culture Collection (FBCC), and the China Center for Type Culture Collection (CCTCC). All strains were cultured under identical conditions for subsequent experiments.

Morphological and physiological characteristics

Colony morphology was observed after 48 h of cultivation at 28 °C on R2A agar plates, with cell morphology further examined using a scanning electron microscope (FEI Quanta 250 FEG; FEI). Antibiotic susceptibility was assessed using the disk diffusion method. Cell suspensions at 0.5 McFarland concentration were prepared from cultures grown on R2A agar. Each strain suspension (80 µL) was spread on R2A agar plates, and the following antibiotic disks were tested (µg per disk): nalidixic acid (30), tetracycline (30), amikacin (30), ampicillin/

sulbactam (20), kanamycin (30), vancomycin (30), chloramphenicol (30), teicoplanin (30), streptomycin (25), gentamicin (30), spectinomycin (25), rifampicin (30), lincomycin (15), and erythromycin (30). Sensitivity was determined by measuring the diameter of inhibition zones, with zones larger than 10 mm considered positive. Growth was tested across a range of temperatures (4–45 °C), pH levels (4.0–14.0, at intervals of 1 pH unit), and NaCl concentrations (0–10%, w/v) using R2A media.

Microbial growth was assessed on eight types of media: Bennett, Luria-Bertani, ISP4, ISP2, R2A, potato dextrose, nutrient, and marine (Difco) agar. Catalase activity was determined by observing bubble formation after treating cells with a 3% (v/v) H_2O_2 solution [22]. Biochemical tests were performed using API 20NE and ZYM kits according to the manufacturer's instructions (bioMérieux).

Biochemical characteristics

For fatty acid profiling, the isolates and three reference strains were cultured on R2A agar media at 28 °C for three days. Cells were harvested during the exponential growth phase and standardized by MIDI (http://www.microbialid.com). Fatty acid profiles were performed using gas chromatography, with results compared to the TSBA6 database. Polar lipids were extracted following the method by Minnikin et al. [23] and identified via two-dimensional thin-layer chromatography (TLC), employing various detection reagents [24].

Phylogenetic analysis

DNA extraction and purification for both strains were performed using the FastDNA™ spin kit for soil (MP Biomedicals). The 16S rRNA genes were amplified by PCR using two universal primers (27F and 1492R) and assembled with SeqMan software (DNASTAR). The sequences were then compared against the EzTaxon database to confirm 16S rRNA-based similarity [25]. Phylogenetic trees were constructed using MEGA (version 11.0) [26] with neighbor-joining (NJ), maximum-likelihood (ML), and maximum-parsimony (MP) algorithms. Evolutionary distances were calculated using Kimura's two-parameter model.

Whole genome sequencing

Genome libraries were prepared using the TruSeq Nano DNA kit and sequenced on the Illumina platform. Illumina sequencing-by-synthesis (SBS) technology, which incorporates individual bases into the DNA template strand via reversible terminators, was employed. Quality control of the raw sequence data from whole-genome sequencing was conducted with FastQC (v0.11.5). Trimmomatic was used to remove adapter sequences and low-quality reads, minimizing potential analysis biases. The base quality plot generated by FastQC was examined to assess overall data quality. Raw data were processed by converting BCL/cBCL files to FASTQ format using bcl2fastq.

Prior to assembly, k-mer analysis was performed to estimate genome size in the sample. De novo assembly was performed using the De Bruijn Graph (DBG) algorithm, with the optimal k-mer selected based on assembly metrics such as contig count, contig sum, and N50. Genome assembly was conducted with SPAdes (v3.15.0) [27], and its quality was evaluated using BUSCO (v3.0.2) [28], which compares the gene content of the genome assembly with expected evolutionary benchmarks. PROKKA (v1.14.6) was then used for genome annotation, including predictions for CDS (Prodigal), rRNA (RNAmmer), and tRNA/tmRNA (Aragorn) [29].

Following assembly, BLAST analysis was applied to identify species most closely matching each scaffold. Best-hit results were determined using the NCBI NT database, and species verification was conducted by comparing Average Nucleotide Identity (ANI) values to reference sequences, applying a 95% similarity threshold. To evaluate bacterial strain relationships, ANI similarity values for 37 *Flavobacterium* genomes were calculated. The whole-genome ANI values were obtained using the ANI/AAI-Matrix (Genome-based distance matrix calculator) [30] and visualized with the *pheatmap* package (1.0.12) in R (4.3.2). Whole-genome taxonomy analysis was performed using the Type Strain Genome Server (TYGS) (http://tygs.dsmz.de) [31] and visualized using the iTOL tool [32].

Genome annotation and comparison

To facilitate genome analysis, we categorized predicted homologous genes into functional categories using the EggNOG database [33]. Draft genomes were annotated through RAST (Rapid Annotation using Subsystem Technology) [34], enabling gene function assignment and identification of various genetic elements. Genome assembly and annotation were conducted using PATRIC (BV-BRC 3.28.5) [35]. Biosynthetic gene clusters (BGCs) related to secondary metabolite production were identified with antiSMASH 7.0 [36], which provided additional annotations using tools like KnownClusterBlast, ClusterBlast, SubClusterBlast, ActiveSiteFinder, and RREFinder. To ensure accuracy in gene function predictions, amino acid sequences of functional genes were aligned and confirmed using NCBI BlastP (https://blast.ncbi.nlm.nih.gov/Blast.cgi).

Multiple sequence alignment for lycopene β-cyclase

Lycopene β-cyclase sequences from reference species were retrieved from NCBI based on BLAST analysis of SUN046_CrtY$_{cd}$ and SUN052_CrtY. Multiple sequence alignments of all lycopene β-cyclases were performed

with Clustal Omega (https://www.ebi.ac.uk/Tools/msa/clustalo/), and alignment results were refined and visualized using Jalview (Jalview 2.11.2.0). Docked structures were analyzed and visualized with BIOVIA Discovery Studio 2024 Client [37].

Carotenoids extraction and detection

Strains SUN046^T and SUN052^T were cultured on R2A agar media to facilitate pigment analysis. After 48 h of growth, colonies were harvested and transferred to centrifuge tubes. Ethanol was added, and the mixture was subjected to 10 min of sonication. The extracts were filtered through a 0.45 µm filter paper and concentrated with a rotary evaporator. The dried extract was weighed and dissolved in ethanol at a final concentration of 1 mg/mL for HPLC analysis, performed using a C18 analytical column (5 µm, stainless steel, 250 mm × 4.6 mm i.d.; Waters). The mobile phase consisted of solvent A (acetonitrile/methanol/water/1 M Tris-HCl) and solvent B (methanol/ethyl acetate) with the following gradient (v/v): starting with 100% solvent A, shifting to 100% solvent B at 19 min, and returning to 100% solvent A at 25 min. The flow rate was set at 1.2 mL/min, with a 20 µL injection volume, and the column was maintained at ambient temperature. Pure carotenoid standards (DHI; Water & Environment) were used as references. HR ESI-MS (High-Resolution Electrospray Ionization Mass Spectrometry) analysis was performed at the Korea Basic Science Institute (KBSI) (Ochang, Center of Research Equipment). For analysis of extracts from SUN046^T and SUN052^T, high-resolution mass spectrometry was performed on a Synapt G2-HDMS mass spectrometer (Waters, Manchester, UK) operated with MassLynx 4.1 software. The extracts were analyzed in positive ion mode with an ESI source, acquiring a mass range of *m/z* 50 to 1,200. Other MS parameters were optimized as follows: capillary voltage of 2.5 kV, cone voltage of 40 V, source temperature of 120 °C, and desolvation gas flow rate of 500 L/h.

Results

Phylogenomic analysis and genomic characteristics

This study aimed to isolate and characterize pigment-producing bacteria from Korean freshwater environments for the potential biotechnological application of microbial pigments in the cosmetic industry. A total of 264 strains exhibiting a broad spectrum of pigmentation (ranging from reddish, pink, purple, and green to yellow, orange, brown, and black) were isolated and taxonomically classified into diverse bacterial lineages. Among these, members of the genus *Flavobacterium* were the most prevalent (14.7%), with all isolates displaying a yellow pigmentation characteristic. To investigate the biosynthesis of yellow pigments in *Flavobacterium*, two novel strains, designated SUN046^T and SUN052^T, were selected for in-depth taxonomic, physiological, and genomic characterization. Blasting of the 16S rRNA gene sequences of SUN046^T and SUN052^T showed highest similarity to *F. chungnamense* KACC 14971^T (96.8%) and *F. aquatile* KACC 11692^T (97.3%), both of which fall below the 98.7% threshold typically used to demarcate bacterial species [38]. In the 16S rRNA phylogenetic tree, constructed using the neighbor-joining method, both strains clustered with *F. koreense* KACC 14969^T, *F. chungnamense* KACC 14971^T and *F. aquatile* KACC 11692^T (Fig. 1A). This clustering pattern was consistent across phylogenetic trees generated with the maximum-likelihood and maximum-parsimony methods (Fig. S1).

Circular graphical maps of the draft genome annotations for strains SUN046^T and SUN052^T are shown in Fig. 1F and G, highlighting the locations of CDS, RNA genes, GC content, virulence factors and antimicrobial resistance genes. The genome of SUN046^T was assembled into 49 contigs, with 33.9% GC content and a total length of 4,140,562 bp. It included 3,452 protein-coding sequences (CDS), 43 transfer RNA (tRNA) genes and 4 ribosomal RNA (rRNA) genes. The genome of SUN052^T was assembled into 33 contigs, comprising 3,363,512 bp with 31.3% GC content. It contained 2,987 CDS, 43 tRNA genes, 3 rRNA genes and 1 transfer-messenger RNA (tmRNA) (Table S1).

Phylogenomic analysis using the TYGS platform indicated that both isolates clustered with *F. aquatile* KACC 11692^T (Fig. 2A), consistent with the 16S rRNA phylogenetic tree. Genetic similarity between strains was assessed by calculating ANI values for the whole genome, which ranged from 76.9 to 81.1%. These ANI values fall below the 95% threshold, supporting sufficient genetic divergence to demonstrate the isolates as novel species (Fig. S2).

Phenotypic and chemotaxonomic characterization

Both strains were aerobic, rod-shaped, non-motile and Gram-negative. Colonies of SUN046^T were light yellow (Fig. 1B) with cells measuring approximately 3.8 × 1.4 µm (Fig. 1C), while SUN052^T colonies were yellow (Fig. 1D) with cell sizes at approximately 1.2 × 0.6 µm (Fig. 1E). Both strains grew well on R2A and nutrient agar but did not grow on Luria-Bertani, ISP4, ISP2, potato dextrose, Bennett and marine agar. Strain SUN046^T grew at temperatures from 10 to 30 °C (optimal at 20 °C), within a pH range of 5.0–7.0 (optimal pH 7.0) and with 0.5–1.0% (w/v) NaCl (optimal 0%). Strain SUN052^T grew from 4 to 30 °C (optimal at 20 °C), at pH 7.0–9.0 (optimal pH 7.0) and tolerated NaCl concentrations of 0.5–1.5% (w/v) (optimal 0%). Both strains exhibited morphological characteristics typical of the *Flavobacterium* genus.

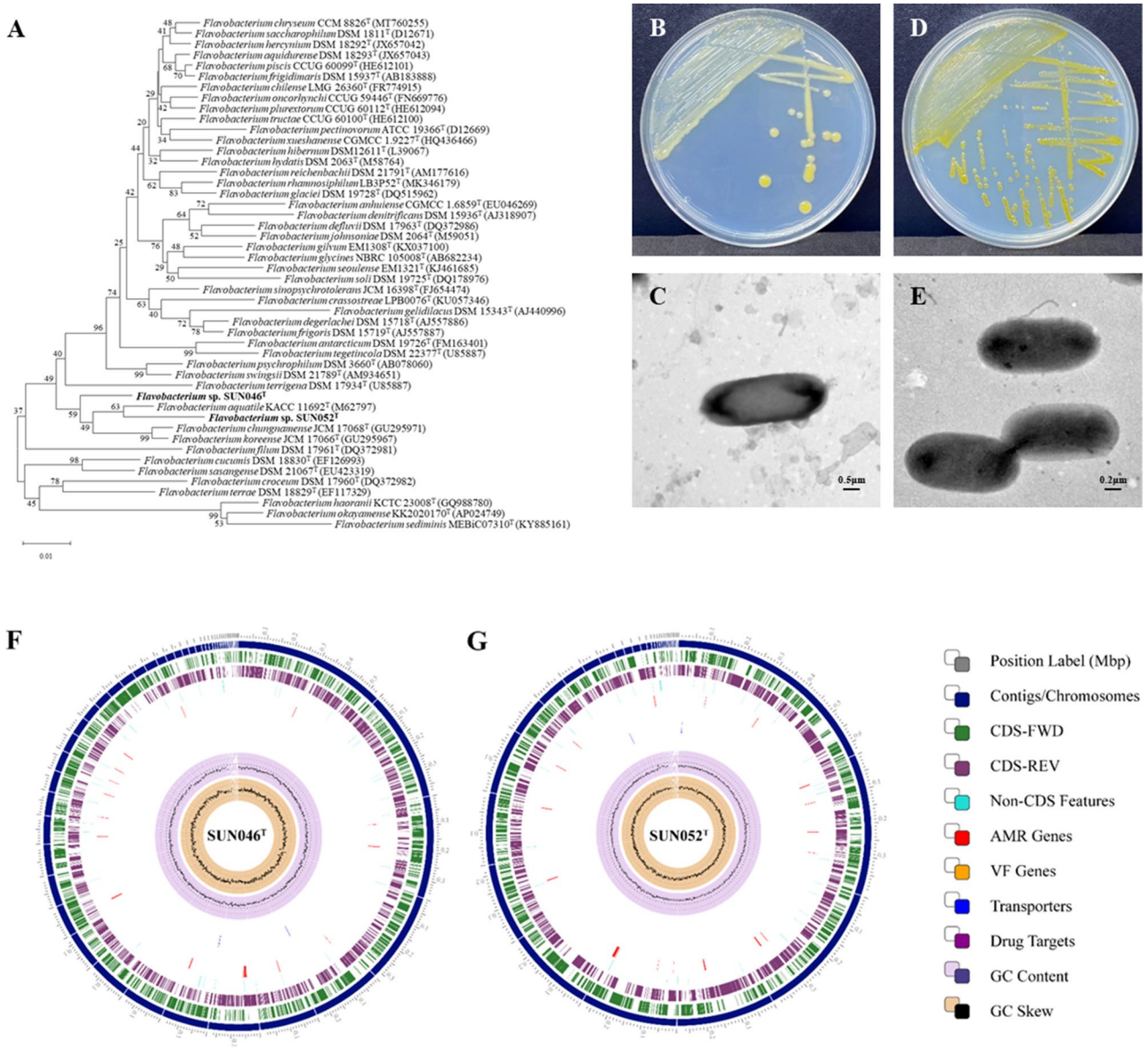

Fig. 1 Phylogenetic tree, morphological characterization, and genome map of strains SUN046^T and SUN052^T. (**A**) Neighbor-joining tree of strains SUN046^T and SUN052^T based on 16S rRNA gene sequences. Bootstrap values > 50% are shown at branch points. Scale bar: 1 nt substitution per 100 nt. Cultivation photos of strains: (**B**) SUN046^T and (**C**) SUN052^T; and scanning electron microscopy images of strains: (**D**) SUN046^T and (**E**) SUN052^T. Circles at branch points represent consensus across various phylogenetic tree-building methods. Circular genome maps of (**F**) SUN046^T and (**G**) SUN052^T display the distribution of genome annotations, arranged from outer to inner rings as follows: contigs, CDS on the forward strand, CDS on the reverse strand, RNA genes, CDS with homology to antimicrobial resistance genes, CDS with homology to virulence factors, GC content, and GC skew

API 20NE results indicated that both strains hydrolyzed esculin, with strain SUN052^T additionally positive for gelatin and β-galactosidase. ZYM test showed that both strains were positive for lipase (C_{14}), trypsin, α-chymotrypsin, α-galactosidase, β-galactosidase, β-glucuronidase, N-acetyl-β-glucosaminidase, α-mannosidase and α-fucosidase, while strain SUN046^T was also positive for β-glucosidase (Table 1). Both strains were sensitive to 14 antibiotics (μg/mL): nalidixic acid (30), tetracycline (30), amikacin (30), ampicillin/sulbactam (20), kanamycin (30), vancomycin (30), chloramphenicol (30), teicoplanin (30), streptomycin (25), gentamicin (30), spectinomycin (25), rifampicin (30), lincomycin (15) and erythromycin (30). Although rifampin resistance genes (*rpoB*) were identified in their genomes, both strains remained sensitive to this antibiotic.

Menaquinone-6 (MK-6) was identified as the predominant menaquinone in both strains. For SUN046^T, the major fatty acids were iso-$C_{15:1}\omega 9c$ (16.9%), summed feature 1 (iso-$C_{15:1}$-H and/or $C_{13:0}$-3OH; 11.5%) and summed feature 5 (ante-$C_{18:0}$ and/or $C_{18:2}\omega 6$, *9c*; 10.9%),

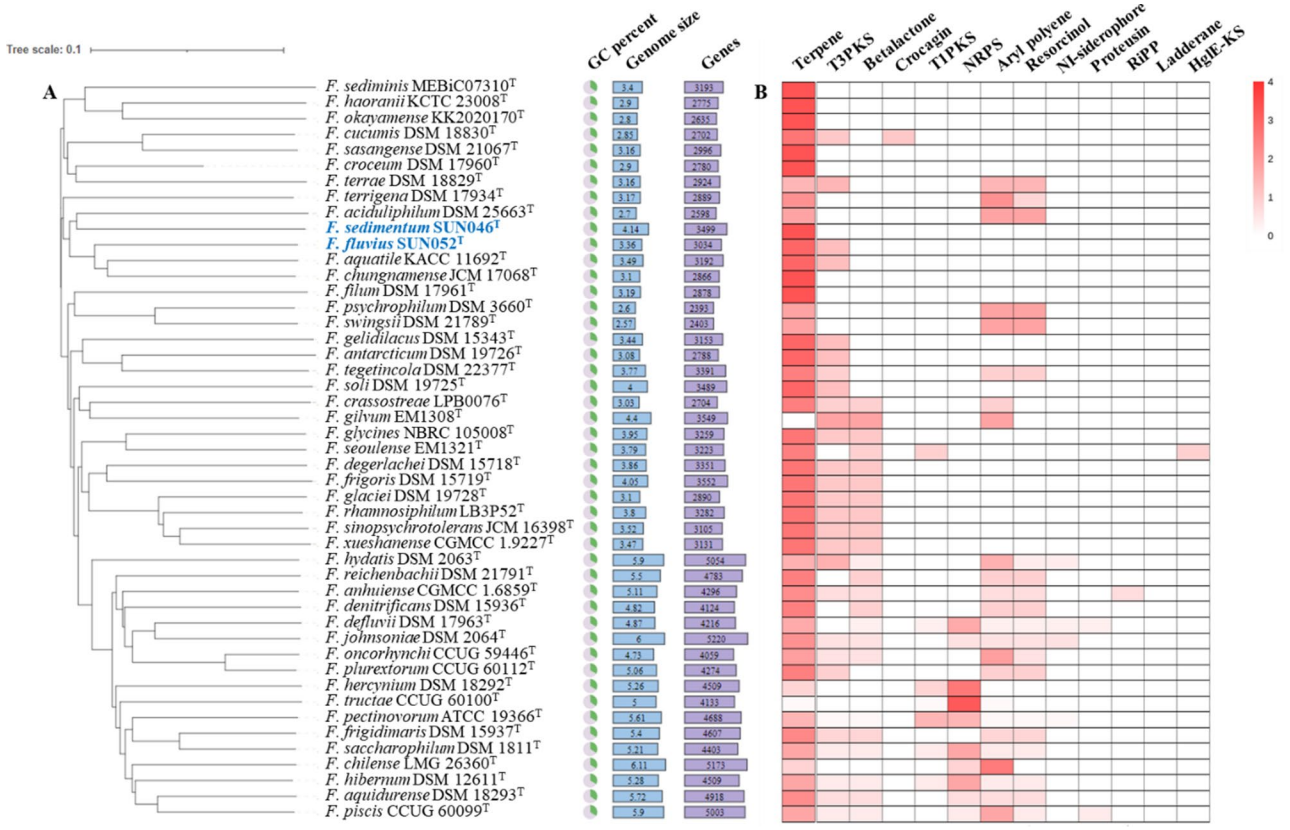

Fig. 2 Phylogenomic tree and genome annotations based on sequence data. (**A**) Genomic tree of isolates (bolded and marked in blue) and related *Flavobacterium* species, generated via TYGS and visualized using iTOL. (**B**) Annotation of secondary metabolites in *Flavobacterium* genomes, analyzed with antiSMASH 7.0. The index represented the number of biosynthetic gene cluster (BGC) types

while SUN052^T predominantly contained $C_{18:1}\omega5c$ (16.3%), iso-$C_{15:1}\omega9c$ (14.3%) and $C_{16:1}\omega11c$ (13.6%). There were qualitative and quantitative differences in the fatty acid profiles between the two strains, particularly in $C_{16:1}\omega9c$, alcohol-$C_{16:1}\omega9c$, summed feature 1 (iso-$C_{15:1}$-H and/or $C_{13:0}$-3OH), summed feature 3 ($C_{16:1}\omega6c$ and/or $C_{16:1}\omega7c$) and summed feature 5 (anteiso-$C_{18:0}$ and/or $C_{18:2}\omega6, 9c$) (Table S2). The polar lipid profile of SUN046^T included one phosphatidyl monomethyl ethanolamine (PME), one phosphatidylethanolamine (PE), nine unidentified amino lipids (AL), one unidentified glycolipid (GL) and two unidentified polar lipids (UL). SUN052^T contained one PE, two ALs, three GLs, two ULs and one unidentified phospholipid (PL) (Fig. S3). Although similar to those reference strains, the polar lipid profiles differed in the quantities of AL, GL, UL and PL.

Based on phenotypic, physiological, chemotaxonomic, and phylogenetic data, we propose that strains SUN046^T and SUN052^T represent novel species within the *Flavobacterium* genus, designated as *Flavobacterium sedimentum* SUN046^T and *Flavobacterium fluvius* SUN052^T, respectively (Table S3).

Genomic annotation and prediction of secondary metabolites

Genome annotation, secondary metabolite prediction and functional gene analysis were conducted using genomic data. Genome annotation was performed with the RAST server, revealing 3,788 coding sequences in strain SUN046^T and 3,024 in strain SUN052^T. Approximately 17% and 21% of these genes, respectively, were annotated within subsystems. Using the EggNOG database for orthology annotation, a total of 1,736 genes in strain SUN046^T were classified into 21 COG categories, while 1,646 genes in strain SUN052^T were assigned to 20 categories.

Secondary metabolite prediction analysis using antiSMASH indicated that SUN046^T possessed only one terpene cluster, whereas SUN052^T contained three biosynthetic gene clusters, including one T3PKS cluster and two distinct terpene clusters (Fig. 2B). Both strains exhibited three major types of terpenes: carotenoid, isorenieratene and (2R,3 S,3'S)-2-hydroxy astaxanthin. Although arylpolyene (APE) pigments were present in roughly half of the *Flavobacterium* species studied, strains SUN046^T and SUN052^T lacked APEs, suggesting that their pigmentation is primarily derived from carotenoids. APE

Table 1 Different characteristics of the novel strains and closely related type strains. Strains: 1, SUN046^T; 2, SUN052^T; 3, *Flavobacterium koreense* KACC 14969^T; 4, *Flavobacterium chungnamense* KACC 14971^T; 5, *Flavobacterium aquatile* KACC 11692^T

Characteristic	1	2	3[a]	4[a]	5[b]
Isolation source	Sediment	Sediment	Cheonho reservoir	Cheonho reservoir	-
Morphology	Rod	Rod	Rod	Rod	Rod
Colony colour	Pale yellow	Yellow	Cream yellow	Cream yellow	Pale yellow
Growth on:					
Nutrient agar	+	+	+	+	-
Tryptic soy agar	-	-	-	-	-
Gliding motility	-	-	-	-	-
Flexirubin-type pigments	-	-	+	+	-
Range of:					
Temperature (℃) (optimum)	10–30 (20)	4–30 (20)	4–37 (25)	10–30 (25)	10–37 (20–30)
pH range (optimum)	5.0–7.0 (7.0)	7.0–9.0 (7.0)	6.0-9.5 (7.0–8.0)	6.5–9.5 (7.5-8.0)	6.5-8.0 (7.0)
NaCl (%, w/v)	0–1 (0)	0-1.5 (0)	0-0.5 (0)	0-0.5 (0)	0-0.5 (0)
Hydrolysis of:					
Esculin	+	+	+	+	+
Gelatine	-	+	+	+	+
β-galactosidase	-	+	-	-	-
Enzymatic activities					
Lipase	+	+	+	+	+
Trypsin	+	+	+	+	+
α-chymotrypsin	+	+	+	+	+
α-galactosidase	+	+	+	+	+
α-mannosidase	+	+	+	+	+
α-fucosidase	+	+	+	+	+
β-galactosidase	+	+	+	+	+
β-glucuronidase	+	+	+	+	+
β-glucosidase	+	-	+	+	+
N-acetyl-β-glucosaminidase	+	+	+	+	+
DNA G+C content (%)	33.9	31.3	31.5	33.2	33.0

* Data from this study. [a] Data from [51]; [b] [52]

pigments, which are yellow and localized in bacterial membranes, help protect against oxidative stress by neutralizing reactive oxygen species. The absence of APEs in SUN046^T and SUN052^T differentiated their pigment composition from strains with APEs, indicating that these two isolates solely relied on carotenoids, which simplified purification and enhanced zeaxanthin isolation efficiency.

Comparative analysis using the PATRIC database showed that strains SUN046^T, SUN052^T and *F. aquatile* KACC 11692^T shared 19 identical antibiotic resistance genes. These genes were categorized as follows: antibiotic targets in susceptible species, regulators modulating antibiotic resistance gene expression, antibiotic target replacement proteins, genes conferring resistance by protein absence and proteins altering cell wall charge to confer antibiotic resistance. Additionally, strains SUN052^T and *F. aquatile* KACC 11692^T contained the *KatG* resistance gene which provides protection against the oxidative burst from phagocytes [39]. For transporter features, all three strains possessed the *GldJ* gene, which is significant for virulence [40]. Strain SUN046^T uniquely contained the oligosaccharide repeat unit polymerase *Wzy*, while proteorhodopsin was present in both SUN052^T and *F. aquatile* KACC 11692^T. Genome annotation from BV-BRC revealed that strain SUN046^T contained CRISPR-related genes (5 CRISPR_Repeat, 4 CRISPR_Spacer and 1 CRISPR_Array), which were absent in strains SUN052^T and *F. aquatile* KACC 11692^T (Table S4).

Carotenoid biosynthesis pathway and Zeaxanthin production

Genome annotation results indicated that strains SUN046^T and SUN052^T possess the MVA pathway for isopentenyl pyrophosphate (IPP) synthesis. Six genes encoding enzymes associated with the MVA pathway were identified in both strains: acetyl-CoA acetyltransferase (ACAT), hydroxymethylglutaryl-CoA synthase (HMGCS), HMG-CoA reductase (HMGCR), mevalonate kinase (MEVK), phosphomevalonate kinase (PMEVK), diphosphomevalonate decarboxylase (DPMVD) and isopentenyl diphosphate isomerase (IDI) (Fig. 3). Notably, strain SUN046^T lacked the HMGCS gene but still retained functionality in the MVA pathway. Similar absences of HMGCS in the MVA pathway were observed in some other *Flavobacterium* species (Table S5), suggesting that a non-homologous enzyme might have substituted for HMGCS, or that an alternative pathway for HMG-CoA synthesis might have been presented in these species.

Both isolates contained four key enzymes involved in the carotenoid biosynthesis pathway: phytoene synthase (CrtB), phytoene dehydrogenase (CrtI), lycopene cyclase (CrtY) and β-carotene hydroxylase (CrtZ). These enzymes catalyze the conversion of geranylgeranyl pyrophosphate (GGPP) to zeaxanthin via lycopene and β-carotene. However, lycopene ε-cyclase (LCYE) and carotene ketolase (CrtW), which are responsible for catalyzing the biosynthesis of lutein from lycopene via α-carotene and astaxanthin from β-carotene via

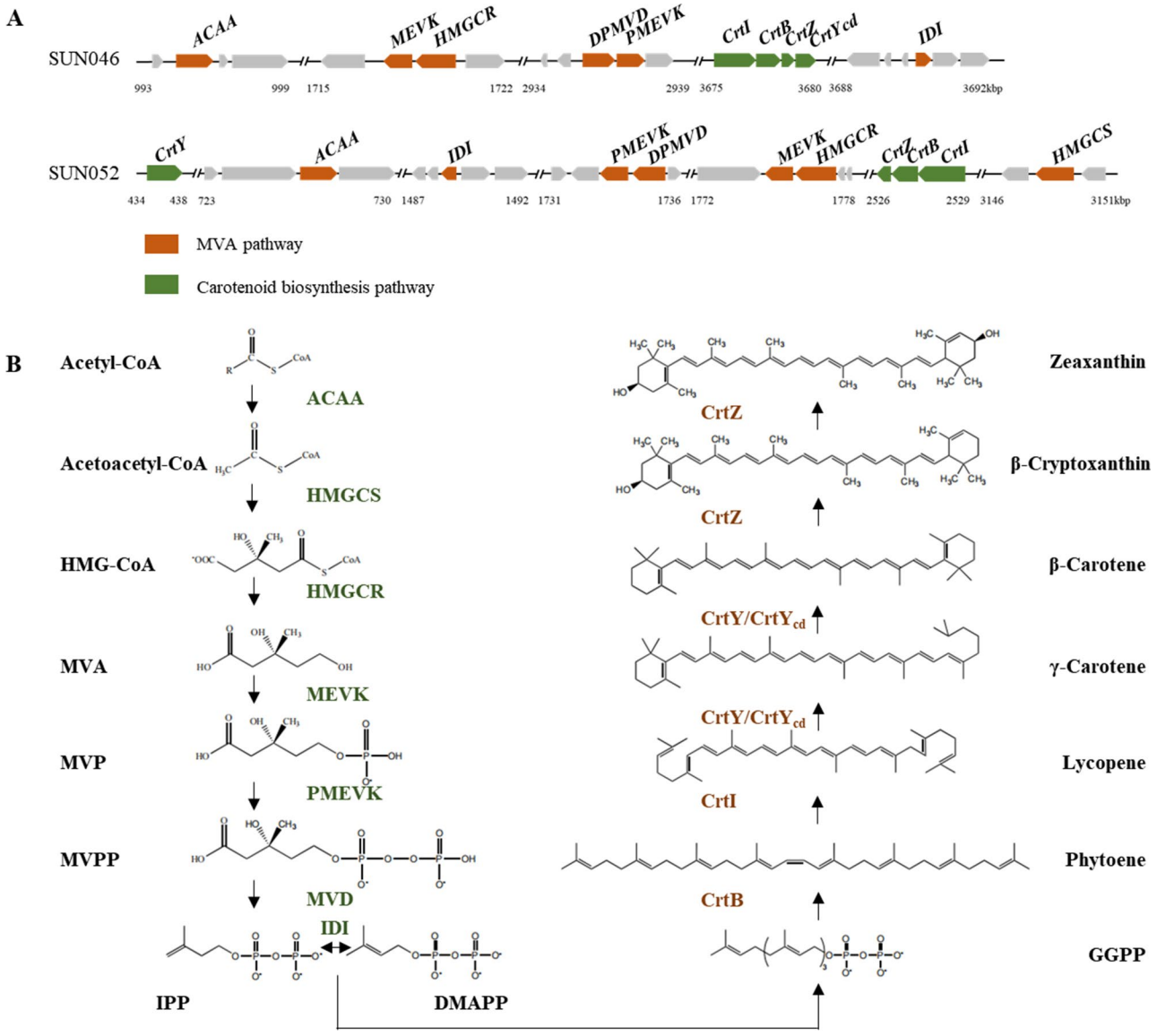

Fig. 3 Proposed MVA (mevalonate) and zeaxanthin biosynthetic pathways in strains SUN046^T and SUN052^T, based on RAST seed annotation and antiSMASH prediction. (**A**) antiSMASH prediction and RAST annotation of gene localization in *Flavobacterium* sp. SUN046^T and SUN052^T. (**B**) The pathway intermediates include acetyl-CoA, acetoacetyl-CoA, HMG-CoA (3-hydroxy-3-methylglutaryl-CoA), MVA, MVP (5-phosphomevalonate), MVPP (5-diphosphomevalonate), IPP (isopentenyl diphosphate), DMAPP (dimethylallyl diphosphate), GGPP (geranylgeranyl pyrophosphate), phytoene, lycopene, γ-carotene, β-carotene, β-cryptoxanthin, and zeaxanthin. Enzymes involved are ACAA (3-ketoacyl-CoA thiolase), HMGCS (hydroxymethylglutaryl-CoA synthase), HMGCR (3-hydroxy-3-methylglutaryl-CoA reductase), MEVK (mevalonate kinase), PMEVK (phosphomevalonate kinase), MVD (diphosphomevalonate decarboxylase), IDI (isopentenyl-diphosphate delta isomerase), CrtB (phytoene synthase), CrtI (phytoene dehydrogenase), CrtY/CrtY$_{cd}$ (lycopene cyclase), and CrtZ (β-carotene hydroxylase)

adonixanthin, were absent. All *Flavobacterium* species contained the *crt* gene cluster, except for *F. gilvum* EM1308^T, which displayed a unique phenotype with a creamy white color [41] in contrast to the typical yellow to orange pigmentation of zeaxanthin-producing *Flavobacterium* species.

The zeaxanthin biosynthesis capability of the isolated strains was evaluated, and yields were quantified via HPLC analysis (Fig. 4). Both strains showed a prominent peak corresponding to zeaxanthin, an unidentified peak, and a trace β-carotene peak in their carotenoid profiles. Zeaxanthin production was further validated by LC-MS/MS analysis (Fig. 4D, E). The zeaxanthin yields of strains. The zeaxanthin yields of strains SUN046^T and SUN052^T were measured as 6.49 μg/mL and 13.23 μg/mL, respectively. Several *Flavobacterium* strains with different zeaxanthin productivity had been reported, as summarized in Table 2. These results indicated that strains SUN046^T and SUN052^T yielded higher levels of zeaxanthin as compared to other *Flavobacterium* species.

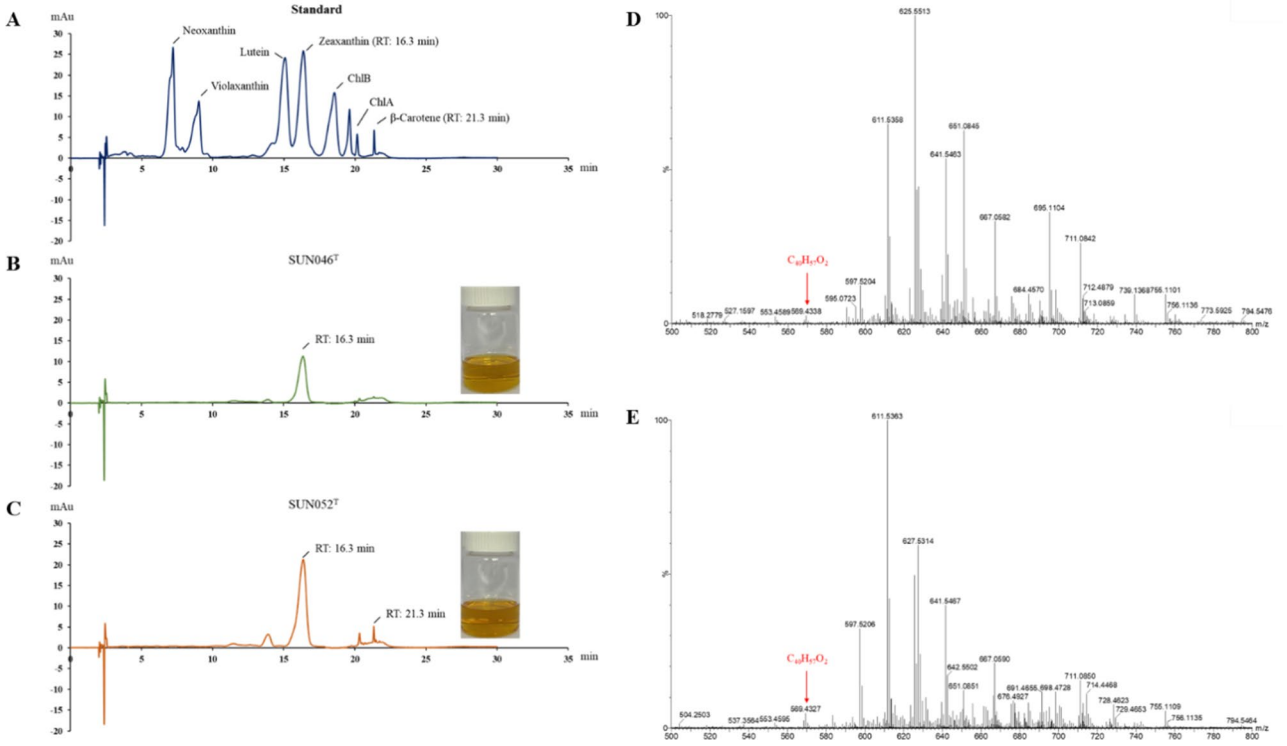

Fig. 4 Carotenoid chromatogram profiles of a standard mixture and the isolates SUN046^T and SUN052^T. (**A**) Standards: neoxanthin (7.183 min), violaxanthin (9.000 min), lutein (15.057 min), zeaxanthin (16.341 min), chlorophyll B (18.528 min), chlorophyll A (20.132 min), and β-carotene (21.325 min). (**B**) Strain SUN046^T: zeaxanthin (16.351 min). (**C**) Strain SUN052^T: zeaxanthin (16.367 min), β-carotene (21.326 min). LC/MS spectra of zeaxanthin ($C_{40}H_{57}O_2$) in strains (**D**) SUN046^T (569.4338 m/z) and (**E**) SUN052^T (569.4327 m/z)

Table 2 Zeaxanthin production by unmodified species in the genus *Flavobacterium*

Strain	Carotenoid	Yield	Reference
F. sedimentum SUN046^T	Zeaxanthin	6.49 μg/mL	This work
F. fluvius SUN052^T	Zeaxanthin	13.23 μg/mL	This work
F. sp. ATCC 25582	Zeaxanthin	0.75 ± 0.03 μg/mL	[53]
F. sp. P8	Zeaxanthin	0.27 ± 0.02 μg/mL	[11]
F. multivorum ATCC 55238^T	Zeaxanthin	9.8 ± 0.09 μg/mL	[54]

Comparison of different types of lycopene cyclase in *Flavobacterium*

Both strains possessed distinct types of lycopene cyclase, referred to as CrtY and CrtY$_{cd}$, respectively. The CrtY type found in strain SUN052^T was commonly observed in bacteria, fungi, algae and plants, whereas the CrtY$_{cd}$ type in strain SUN046^T was rarely found in only 5 out of 45 species in the *Flavobacterium* genus (Fig. 5A and Table S1). To explore the functional and mechanistic differences due to structural variations between CrtY and CrtY$_{cd}$, we conducted amino acids alignment, 3D structure prediction, and molecular docking analysis with relevant substrates.

A distinct pattern in the amino acid sequence of CrtY was noted between the two isolates. Sequence alignment of SUN046_CrtY$_{cd}$ showed significant conservation with the N-terminal domain of CrtYB, arising from a concatenated fusion involving the *crtY*$_c$-*crtY*$_d$ and *crtB* genes [42]. A key feature within these domains was the highly conserved PXE(E/D) motif (Fig. 5C) which served as an active site. This motif was a universal signature in this class of lycopene β-cyclases, found across archaea, fungi and bacteria, underscoring its importance in enzymatic function [43]. The conservation of this motif in various cyclases suggested a central role in the catalytic mechanism.

In contrast, sequence alignment of SUN052_CrtY and other bacterial CrtY types revealed N- and C-terminal deletions compared with plant and cyanobacterial LCYBs. Conserved regions were identified not only in the lycopene cyclases (LCY) of other bacteria and plants but also in SUN052_CrtY. Analysis of conserved motifs highlighted the presence of a dinucleotide-binding domain, an LCY-specific motif, cyclase motifs 1 and 2, along with three β-LCY CAD regions (Catalytic Activity Domains) which were essential for lycopene cyclase's enzymatic activity [44]. Orthologous proteins such as CrtY in bacteria and CrtL (including CrtL-b and LCY-b) in cyanobacteria, algae and higher plants exhibited substantial structural homology, containing NAD(P)/FAD binding motifs [42]. Within these conserved sequences, the motif V/IXGXGXXGXXXA (highlighted in red, Fig. 5B) was associated with FAD/NAD cofactor binding.

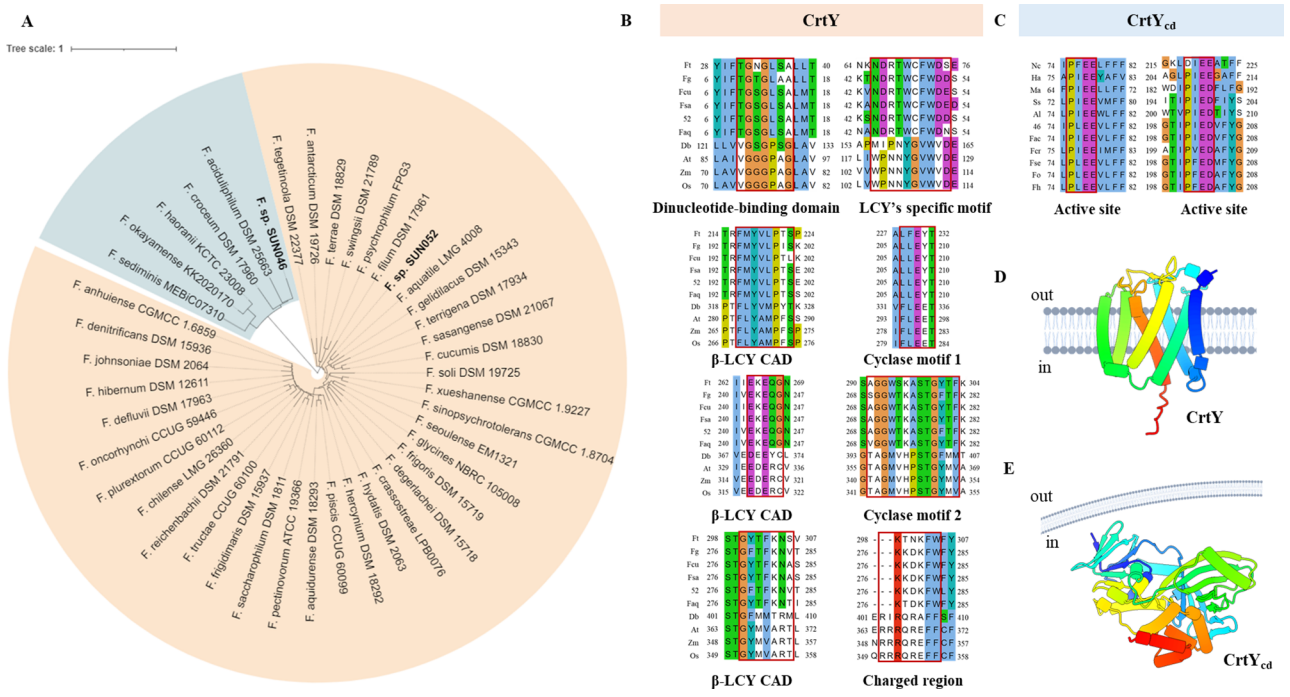

Fig. 5 Phylogenetic analysis and sequence alignment of lycopene β-cyclases in *Flavobacterium*. (**A**) Phylogenetic tree of *crtY* and *crtY*$_{cd}$ genes constructed using MEGA 6.0. (**B**) Characteristic regions of CrtY and LCYB, marked below the LCYB sequence: dinucleotide binding site, LCY-specific motif, cyclase motifs 1 and 2, charged region and β-LCY CAD (catalytically active domain). (**C**) Two active sites of CrtY$_{cd}$. (D) and (E) Structural variations in lycopene β-cyclase in SUN046^T (CrtY$_{cd}$) and SUN052^T (CrtY)

Additionally, a glutamic acid residue within the conserved FLEET motif was critical for β-carotene biosynthesis [44].

We further analyzed lycopene β-cyclases for potential membrane or cytosolic localization by predicting membrane helices using DeepTMHMM. Three distinct types of lycopene β-cyclases were identified and tested: cytosolic lycopene β-cyclase type (CrtY, LYC), membrane-bound lycopene β-cyclase (CrtY$_{cd}$) and bifunctional CrtY/CrtB-type (Fig. 5D and Table S1). To achieve a comprehensive understanding of how these conserved regions contributed to enzymatic activity, we conducted an in-depth examination of the 3D structural models.

Molecular docking studies provided deeper insights into the binding of lycopene with different CrtY$_{cd}$ and CrtY types. The binding affinity of SUN046_CrtY$_{cd}$ and SUN052_CrtY with lycopene and FAD was recorded as -11 and − 9.4 kcal/mol, respectively. The cavity volumes (Å^3) of the two enzymes were 960 and 2,335, with the binding site coordinates at (5, -1, -4) and (4, 7, 3), respectively, pinpointing precise locations within the protein structures. Key residues involved in SUN046_CrtY$_{cd}$ included PRO (75, 201), LEU (76, 202) and GLU (77, 78, 203, 204). For SUN052_CrtY, the FAD-binding site involved key residues GLY (10, 12) and ALA15, consistent with the conserved motifs in the amino acid alignment (Table S6).

Discussion

In this study, we successfully identified and classified two novel species *F. sedimentum* SUN046^T and *F. fluvius* SUN052^T through a polyphasic taxonomic approach. Comparative genomic analysis with 45 closely related *Flavobacterium* species provided insights into the genetic and evolutionary diversity of zeaxanthin biosynthesis, particularly focusing on lycopene β-cyclase within the *Flavobacterium* genus.

Along with other *Flavobacterium* species, both isolates only utilized the MVA pathway for IPP synthesis, whereas most bacteria and plastids typically employed the 2-C-methyl-D-erythritol 4-phosphate (MEP) and/or partial MVA pathways. The MVA pathway generally encompassed two different types which were from eukaryotic or archaeal (modified). In the modified MVA pathway, certain enzymes, particularly phosphomevalonate kinase (PMK) and diphosphomevalonate decarboxylase (DMD) in the lower pathway (from mevalonate to IPP synthesis), were replaced by non-homologous enzymes or similar reactions to complete the pathway [45]. While enzyme replacements in the lower MVA pathway had been documented in archaea and *Chloroflexi* bacteria, the absence of enzymes in the upper MVA pathway (up to mevalonate synthesis) was rarely observed [46]. Comparative genomic analysis revealed that HMG-CoA synthase (HMGCS) was absent in SUN046^T and other

Flavobacterium species among the 45 examined (Table S1). These findings suggested that *Flavobacterium* species may have acquired an incomplete MVA pathway through horizontal gene transfer from eukaryotic or archaeal sources, potentially representing another type of modified MVA pathway. Further genetic studies are warranted to identify non-homologous enzymes that may replace HMGCS in strain SUN046^T and some of the *Flavobacterium* species.

Genome annotations results revealed that *crtY* and *crtY*$_{cd}$ genes were presented across the *Flavobacterium* genus, though the *crtY*$_{cd}$ gene was only found in six strains, including SUN046^T (Table S1). Interestingly, *crtY*$_{cd}$ in these strains showed high sequence homology with genes from archaea and fungi (Fig. S4). This observation aligned with previous studies of describing the unique structural features of the *crtY*$_{cd}$ gene in archaea, which includes a fusion of *crtY*$_c$ and *crtY*$_d$ domains connected by an additional transmembrane segment [47]. This domain arrangement may be an adaptation to the distinct environmental conditions in archaea. In fungi, the presence of *crtYB* reflected a further fusion of *crtY*$_{cd}$ and *crtB* genes [43], suggesting evolutionary innovation. Additionally, the CrtY in strain SUN052^T displayed amino acid sequence conservation with LCY from microalgae and plants, indicating that these organisms shared a common phylogenetic origin and retained an ancient genetic connection [48].

The differences in ligand-binding modes and catalytic domain structures between CrtY and CrtY$_{cd}$ implied that distinct catalytic mechanisms might have affected carotenoid biosynthesis efficiency (Fig. S4). The CrtY sequence contained multiple catalytic domains and cyclase motifs, whereas CrtY$_{cd}$ had only two catalytic domains. The production of zeaxanthin in strain SUN052^T was approximately twice of SUN046^T. This correlation between catalytic domain abundance and zeaxanthin biosynthesis efficiency was further supported by 3D protein structure analysis, which showed more β-strands in the structure of strain SUN052^T (Table S6). The increased number of β-strand might contribute to additional active sites, potentially enhancing the carotenoid production capacity of this strain [49]. However, further studies are needed to explore the influence of the differing position of promoters in crtY and crtYcd in SUN052^T and SUN046^T on zeaxanthin yield. In crtY$_{cd}$ of SUN046^T, the *crt* gene cluster is arranged as an operon (*crtI-crtB-crtZ-crtY*$_{cd}$), regulated by a single promoter for the entire gene cluster. In contrast, crtY in SUN052^T is positioned separately from the *crt* operon, which may allow for more robust expression, regardless of the promoter distance (Fig. S5).

Lycopene β-cyclase had attracted great interest owe to its role in promoting high-value carotenoid production across various organisms. Overexpression of the *crtY* gene had significantly increased lycopene production in *E. coli* through advanced genetic modifications [50]. This approach had also been applied to plants like tomato, *Arabidopsis* and sweet potato, demonstrating that *crtY* could enhance resistance to environmental stresses, including drought and salinity [55]. Although the importance of lycopene β-cyclase in carotenoid biosynthesis is well recognized, our study is the first to conduct a comparative genomic analysis of structural variations in lycopene β-cyclase and the carotenoid biosynthesis pathway within *Flavobacterium* species. The identified crtY and crtY$_{cd}$ in these two novel *Flavobacterium* species represent promising targets for metabolic and protein engineering, and have the potential to improve the enzyme activity for zeaxanthin production in future studies.

Conclusion

This study provides valuable insights into the carotenoid biosynthetic and genetic diversity of *Flavobacterium* strains. Two novel species, SUN046^T and SUN052^T, display distinct zeaxanthin biosynthetic pathways, highlighting their potential for biotechnological applications. Notably, the absence of APE pigments in these strains streamlines the purification process, enhancing the efficiency of zeaxanthin extraction and making them as promising candidates for industrial-scale production. Future research needs to explore the functional properties of these variants, their applicability in various organisms and innovative strategies to utilize their biosynthetic capabilities for sustainable and efficient zeaxanthin production.

Abbreviations

ACAA	3-Ketoacyl-CoA thiolase
HMGCS	Hydroxymethylglutaryl-CoA Synthase
HMGCR	3-hydroxy-3-Methylglutaryl-CoA Reductase
MEVK	Mevalonate Kinase
PMEVK	Phosphomevalonate Kinase
DPMVD	Diphosphomevalonate Decarboxylase
IDI	Isopentenyl-Diphosphate Delta Isomerase
CrtB	Phytoene Synthase
CrtI	Phytoene Dehydrogenase
CrtY	Lycopene Cyclase
CrtZ	β-Carotene Hydroxygease

Supplementary Information

The online version contains supplementary material available at https://doi.org/10.1186/s12866-025-03954-0.

Supplementary Material 1

Acknowledgments

We gratefully acknowledge the initial support provided by the Korea Environment Industry & Technology Institute (KEITI) through a project (2021003240004) funded by the Korea Ministry of Environment (MOE), focused on the development of eco-friendly materials and processing technologies derived from wildlife.

Author contributions
H.-G. L, Y.Z. and C. J. conceived and designed the project. Y.Z. and C. J.: Data curation, Formal analysis, Investigation, Methodology, Visualization, Writing. C.-S. L. and K.-S. S.: Investigation, Validation, Writing – review & editing. H.-G. L: Supervision, Writing – review & editing. All the authors contributed to manuscript revision and approved the final manuscript.

Funding
This work was supported by the Korea Environment Industry & Technology Institute (KEITI), through the project to advance the multi-ministerial national biological research resources funded by the Korea Ministry of the Environment (MOE) (2021003420002) and supported by IPET through the Agricultural Machinery/Equipment Localization Technology Development Program funded by MAFRA (321056-5). This work was also supported by the National Research Council of Science & Technology (Grant No. CAP20024-200) of the Korea government (MSIT).

Data availability
The authors confirm that the data supporting the findings of this study are available within the article and supplementary materials. Whole genome sequences obtained in this study have been deposited in the NCBI with the accession numbers: JAPQNT000000000 and JAPQNS000000000O.

Declarations

Ethics approval and consent to participate
Not applicable.

Consent for publication
Not applicable.

Competing interests
The authors declare no competing interests.

Received: 16 January 2025 / Accepted: 7 April 2025
Published online: 23 April 2025

References

1. Liang M-H, Xie S-R, Dai J-L, Chen H-H, Jiang J-G. Roles of two phytoene synthases and orange protein in carotenoid metabolism of the β-Carotene-Accumulating *Dunaliella salina*. Microbiol Spectr. 2023;11:e00069–23.
2. Ziegelhoffer EC, Donohue TJ. Bacterial responses to photo-oxidative stress. Nat Rev Microbiol. 2009;7:856–63.
3. Pérez-Gálvez A, Viera I, Roca M. Carotenoids and chlorophylls as antioxidants. Antioxidants. 2020;9:505.
4. Hayashi M, Naknukool S, Hayakawa S, Ogawa M, Ni'matulah A-BA. Enhancement of antimicrobial activity of a lactoperoxidase system by Carrot extract and β-carotene. Food Chem. 2012;130:541–6.
5. Bolhassani A, Khavari A, Bathaie SZ. Saffron and natural carotenoids: biochemical activities and anti-tumor effects. Biochimica et biophysica acta (BBA) -. Reviews Cancer. 2014;1845:20–30.
6. Park H-A, Hayden MM, Bannerman S, Jansen J, Crowe-White KM. Anti-Apoptotic effects of carotenoids in neurodegeneration. Molecules. 2020;25:3453.
7. Hira S, Saleem U, Anwar F, Sohail MF, Raza Z, Ahmad B. β-Carotene: A natural compound improves cognitive impairment and oxidative stress in a mouse model of Streptozotocin-Induced Alzheimer's disease. Biomolecules. 2019;9:441.
8. Zhang Y, Liu Z, Sun J, Xue C, Mao X. Biotechnological production of Zeaxanthin by microorganisms. Trends Food Sci Technol. 2018;71:225–34.
9. Roll Zimmer TB, Barboza Mendonça CR, Zambiazi RC. Methods of protection and application of carotenoids in foods - A bibliographic review. Food Bioscience. 2022;48:101829.
10. Barreiro C, Barredo J-L, editors. Microbial carotenoids: methods and protocols. New York, NY: Springer New York; 2018.
11. Vila E, Hornero-Méndez D, Lareo C, Saravia V. Biotechnological production of Zeaxanthin by an Antarctic *Flavobacterium*: evaluation of culture conditions. J Biotechnol. 2020;319:54–60.
12. Bing-Chung Liau S-EH, Hong S-E, Chang L-P, Shen C-T, Li Y-C, Wu Y-P, et al. Separation of sight-protecting Zeaxanthin from Nannochloropsis oculata by using supercritical fluids extraction coupled with elution chromatography. Sep Purif Technol. 2011;78:1–8.
13. Hsu Y-W, Tsai C-F, Chen W-K, Ho Y-C, Lu F-J. Determination of lutein and Zeaxanthin and antioxidant capacity of supercritical carbon dioxide extract from daylily (Hemerocallis disticha). Food Chem. 2011;129:1813–8.
14. Bergey DH, Harrison FC, Breed RS, Hammer BW. F.M. Huntoon. Manual of determinative bacteriology. Baltimore, USA: Williams and Wilkins; 1923.
15. Dong K, Xu B, Zhu F, Wang G. Flavobacterium hauense Sp. nov., isolated from soil and emended descriptions of Flavobacterium subsaxonicum, Flavobacterium beibuense and Flavobacterium rivuli. Int J Syst Evol MicroBiol. 2013;63(Pt9):3237–42.
16. Kang JY, Chun J, Jahng KY. *Flavobacterium aciduliphilum* Sp. nov., isolated from freshwater, and emended description of the genus *Flavobacterium*. Int J Syst Evol MicroBiol. 2013;63 Pt5:1633–8.
17. Kuo I, Saw J, Kapan DD, Christensen S, Kaneshiro KY, Donachie SP. *Flavobacterium akiainvivens* sp. nov., from decaying wood of Wikstroemia oahuensis, Hawai'i, and emended description of the genus *Flavobacterium*. International Journal of Systematic and Evolutionary Microbiology. 2013;63 Pt_9:3280–6.
18. Bernardet J-F, Segers P, Vancanneyt M, Berthe F, Kersters K. basonym, Cytophaga aquatilis Strohl and Tait. Cutting a gordian knot: Emended classification and description of the genus *Flavobacterium*, emended description of the family *Flavobacteriaceae*, and proposal of *Flavobacterium hydatis* nom nov (1978).
19. Tao L, Yao H, Kasai H, Misawa N, Cheng Q. A carotenoid synthesis gene cluster from *Algoriphagus* Sp. KK10202C with a novel fusion-type lycopene β-cyclase gene. Mol Genet Genomics. 2006;276:79–86.
20. Göttl VL, Pucker B, Wendisch VF. Screening of structurally distinct lycopene β-Cyclases for production of the Cyclic C40 carotenoids β-Carotene and Astaxanthin by *Corynebacterium glutamicum*. J Agric Food Chem. 2023;71:7765–76.
21. Nakajima Y, Tsukamoto T, Kumagai Y, Ogura Y, Hayashi T, Song J, et al. Presence of a haloarchaeal Halorhodopsin-Like Cl^- pump in marine Bacteria. Microbes Environ. 2018;33:89–97.
22. Kovacs N. Identification of *Pseudomonas pyocyanea* by the oxidase reaction. Nature. 1956;178:703–703.
23. Minnikin DE, O'Donnell AG, Goodfellow M, Alderson G, Athalye M, Schaal A, et al. An integrated procedure for the extraction of bacterial isoprenoid Quinones and Polar lipids. J Microbiol Methods. 1984;2:233–41.
24. Komagata K, Suzuki K-I. 4 Lipid and Cell-Wall analysis in bacterial systematics. Methods in microbiology. Elsevier; 1988. pp. 161–207.
25. Jin C-Z, Song X, Sung YJ, Jin F-J, Li T, Oh H-M, et al. *Lysobacter profundi* Sp. Nov., isolated from freshwater sediment and reclassification of *Lysobacter panaciterrae* as *Luteimonas panaciterrae* comb. Nov. Int J Syst Evol MicroBiol. 2020;70:3878–87.
26. Tamura K, Stecher G, Kumar S. MEGA11: molecular evolutionary genetics analysis version 11. Mol Biol Evol. 2021;38:3022–7.
27. Bankevich A, Nurk S, Antipov D, Gurevich AA, Dvorkin M, Kulikov AS, et al. SPAdes: A new genome assembly algorithm and its applications to Single-Cell sequencing. J Comput Biol. 2012;19:455–77.
28. Simão FA, Waterhouse RM, Ioannidis P, Kriventseva EV, Zdobnov EM. BUSCO: assessing genome assembly and annotation completeness with single-copy orthologs. Bioinformatics. 2015;31:3210–2.
29. Seemann T. Prokka: rapid prokaryotic genome annotation. Bioinformatics. 2014;30:2068–9.
30. Rodriguez -RLM, Konstantinidis KT. The enveomics collection: a toolbox for specialized analyses of microbial genomes and metagenomes. Preprint. PeerJ Preprints; 2016.
31. Meier-Kolthoff JP, Göker M. TYGS is an automated high-throughput platform for state-of-the-art genome-based taxonomy. Nat Commun. 2019;10:2182.
32. Letunic I, Bork P. Interactive tree of life (iTOL) v5: an online tool for phylogenetic tree display and annotation. Nucleic Acids Res. 2021;49:W293–6.
33. Huerta-Cepas J, Forslund K, Coelho LP, Szklarczyk D, Jensen LJ, Von Mering C, et al. Fast Genome-Wide functional annotation through orthology assignment by eggNOG-Mapper. Mol Biol Evol. 2017;34:2115–22.
34. Aziz RK, Bartels D, Best AA, DeJongh M, Disz T, Edwards RA, et al. The RAST server: rapid annotations using subsystems technology. BMC Genomics. 2008;9:75.
35. Wattam AR, Davis JJ, Assaf R, Boisvert S, Brettin T, Bun C, et al. Improvements to PATRIC, the all-bacterial bioinformatics database and analysis resource center. Nucleic Acids Res. 2017;45:D535–42.

36. Blin K, Shaw S, Augustijn HE, Reitz ZL, Biermann F, Alanjary M, et al. AntiSMASH 7.0: new and improved predictions for detection, regulation, chemical structures and visualisation. Nucleic Acids Res. 2023;51:W46–50.
37. Kadiri M, Sevugapperumal N, Nallusamy S, Ragunathan J, Ganesan MV, Alfarraj S, et al. Pan-genome analysis and molecular Docking unveil the biocontrol potential of *Bacillus velezensis* VB7 against *Phytophthora infestans*. Microbiol Res. 2023;268:127277.
38. Jo H, Park MS, Lim Y, Kang I, Cho J-C. Ten Novel Species Belonging to the Genus *Flavobacterium*, Isolated from Freshwater Environments: *F. praedii* sp. nov., *F. marginilacus* sp. nov., *F. aestivum* sp. nov., *F. flavigenum* sp. nov., *F. luteolum* sp. nov., *F. gelatinilyticum* sp. nov., *F. aquiphilum* sp. nov., *F. limnophilum* sp. nov., *F. lacustre* sp. nov., and *F. eburneipallidum* sp. nov. J Microbiol. 2023;61:495–510.
39. Tekedar HC, Karsi A, Reddy JS, Nho SW, Kalindamar S, Lawrence ML. Comparative genomics and transcriptional analysis of *Flavobacterium columnare* strain ATCC 49512. Front Microbiol. 2017;8.
40. Thunes NC, Evenhuis JP, Lipscomb RS, Pérez-Pascual D, Stevick RJ, Birkett C, et al. Gliding motility proteins GldJ and SprB contribute to *Flavobacterium columnare* virulence. J Bacteriol. 2024;206:e00068–24.
41. Shin S-K, Ha Y, Cho Y-J, Kwon S, Yong D, Yi H. *Flavobacterium gilvum* Sp. nov., isolated from stream water. Int J Syst Evol MicroBiol. 2017;67:153–7.
42. Zhao Z, Liu Z, Mao X. Biotechnological advances in lycopene β-Cyclases. J Agric Food Chem. 2020;68:11895–907.
43. Peck RF, Johnson EA, Krebs MP. Identification of a lycopene β-Cyclase required for bacteriorhodopsin biogenesis in the archaeon *Halobacterium salinarum*. J BACTERIOL. 2002;184.
44. Fang H, Liu J, Ma R, Zou Y, Ho S-H, Chen J, et al. Functional characterization of lycopene β- and ε-Cyclases from a Lutein-Enriched green microalga *Chlorella sorokiniana* FZU60. Mar Drugs. 2023;21:418.
45. Lombard J, Moreira D. Origins and early evolution of the mevalonate pathway of isoprenoid biosynthesis in the three domains of life. Mol Biol Evol. 2011;28:87–99.
46. Hayakawa H, Motoyama K, Sobue F, Ito T, Kawaide H, Yoshimura T, et al. Modified mevalonate pathway of the archaeon *Aeropyrum pernix* proceeds via *trans* -anhydromevalonate 5-phosphate. Proc Natl Acad Sci USA. 2018;115:10034–9.
47. Cheng Q. Structural diversity and functional novelty of new carotenoid biosynthesis genes. J IND MICROBIOL BIOTECHNOL. 2006;33:552–9.
48. Krubasik P, Sandmann G. Molecular evolution of lycopene cyclases involved in the formation of carotenoids with ionone end groups. Biochem Soc Trans. 2000;28.
49. Marcos E, Basanta B, Chidyausiku TM, Tang Y, Oberdorfer G, Liu G, et al. Principles for designing proteins with cavities formed by curved B sheets. Science. 2017;355:201–6.
50. Li M, Xia Q, Zhang H, Zhang R, Yang J. Metabolic engineering of different microbial hosts for lycopene production. J Agric Food Chem. 2020;68:14104–22.
51. Lee S, Weon H-Y, Kim S-J, Ahn T-Y. *Flavobacterium koreense* Sp. nov., *Flavobacterium chungnamense* Sp. nov., and *Flavobacterium cheonanense* Sp. nov., isolated from a freshwater reservoir. J Microbiol. 2011;49:387–92.
52. Sheu S-Y, Lin Y-S, Chen W-M. *Flavobacterium squillarum* sp. nov., isolated from a freshwater shrimp culture pond, and emended descriptions of *Flavobacterium haoranii*, *Flavobacterium cauense*, *Flavobacterium terrae* and *Flavobacterium aquatile*. International Journal of Systematic and Evolutionary Microbiology. 2013;63 Pt_6:2239–47.
53. Alcantara S, Sanchez S. Influence of carbon and nitrogen sources on *Flavobacterium* growth and Zeaxanthin biosynthesis. J Ind Microbiol Biotechnol. 1999;23:697–700.
54. Bhosale P, Larson AJ, Bernstein PS. Factorial analysis of Tricarboxylic acid cycle intermediates for optimization of Zeaxanthin production from *Flavobacterium multivorum*. J Appl Microbiol. 2004;96:623–9.
55. Kang C, Zhai H, Xue L, Zhao N, He S, Liu Q. A lycopene β-cyclase gene, IbLCYB2, enhances carotenoid contents and abiotic stress tolerance in transgenic sweetpotato. Plant Sci. 2018;272:242–54.

Publisher's note